metals

MDPI

Article

Flow Stress of bcc Metals over a Wide Range of Temperature and Strain Rates

Gabriel Testa, Nicola Bonora *, Andrew Ruggiero and Gianluca Iannitti

Department of Civil and Mechanical Engineering, University of Cassino and Southern Lazio, I-03043 Cassino, Italy; gabriel.testa@unicas.it (G.T.); andrew.ruggiero@unicas.it (A.R.); gianluca.iannitti@unicas.it (G.I.)

* Correspondence: nicola.bonora@unicas.it; Tel.: +39-0776-299-3693

Received: 25 November 2019; Accepted: 9 January 2020; Published: 13 January 2020

Abstract: A physical-based model for the flow stress of bcc metals is presented. Here, thermally activated and viscous drag regimes are considered. For the thermally activated component of the flow stress, the diffusion-controlled regime at elevated temperature is also taken into account assuming the non-linear dependence of the activation volume on temperature. The model was applied to A508 (16MND5) steel showing the possibility to accurately describe the variation of the flow stress over the entire temperature range (from 0 K to T_m) and over a wide strain-rate range.

Keywords: flow stress; activation volume; strain rate; temperature; bcc

1. Introduction

Today, numerical simulation tools have the potential to anticipate the performance of components and systems under varying operational scenarios, dramatically reducing the need for verification experiments and accelerating the engineering design process [1]. For what concerns the mechanical response is that the reliability of such predictive approach relies on the accuracy of material constitutive models used in the simulations. In many industrial sectors, such as defense, aerospace, oil and gas, automotive and manufacturing engineering applications, there is an increasing demand for models capable to describe material behavior under complex load paths involving large inelastic deformation and failure under different strain rate and temperature conditions. Over the past hundred years, modelling of deformation of metals and alloys has been largely investigated. A review of non-linear constitutive models can be found in [2,3]. For what concern the material yield stress is that the classical rate-independent plasticity theories represent idealizations which in general have limited applicability. Macroscopic constitutive formulations can be categorized into two main groups: phenomenological constitutive relationships and physical-based models. Models that fall in the first group are mathematical formulations for the material flow stress as a function of plastic strain, strain rate, and temperature, which are developed based on the empirical observations. Usually, these mathematical expressions fit the experimental data but not necessarily address any specific deformation mechanism. They require few material constants that can be determined easily by fitting or inverse calibration of simple tensile or compression test data. Since the mathematical expression of the flow stress is given in explicit form, its implementation in the finite element method (FEM) code is straightforward. Nowadays, many of these models are readily available in the material library of commercial FEM software. Examples of these type of models are Cowper and Symonds [4], Johnson and Cook [5], and Bodner and Partom [6]. The main limitation of these formulations is that they work well only over a limited range of variability of the constitutive variables (i.e., plastic strain, strain rate, and temperature) over which model parameters are determined. Plastic deformation in metals, which deform through dislocations motion and accumulation, is in general a rate- and temperature-dependent process [7]. The motion of dislocations through the crystals of a polycrystalline

alloy is a complex phenomenon with various features which cannot be described by simple mathematical models. Physical-based models are derived considering the micromechanics of plastic deformation and are based on the thermally activated motion of dislocations [8]. These models usually can predict fairly well as material behavior over a much wider range of variability of strain, strain rate, and temperature, but they require a larger number of material constants that have physical meaning but are more challenging to be determined. Examples of such type of models can be found in Kocks et al. [9], Follansbee and Kocks [10], Nemat-Nasser and Li [7], and Voyiadjis and Abed [11].

Probably the feature that most distinguishes bcc pure metals and alloys from their fcc and hcp counterparts is the strong temperature dependence of the yield and flow stresses at low temperatures and its related effect on slip geometry [12]. Modelling the yield stress for these class of metals over a wide range of temperature and strain rates is a challenge. Cosrad [13] investigated the variation of the yield stress at low temperature in bcc polycrystals metals and alloys. In particular, he observed that the temperature sensitivity of the yield stress in iron increases with grain boundary and interstitial impurities. Kawata et al. [14] investigated strain rate effect on ductility in bcc and fcc metals. Zerilli and Armstrong [15] proposed a dislocation-mechanics-based constitutive relations for bcc and fcc metals based on the observation that in bcc metals the activation volume is essentially independent of plastic strain while in fcc metals thermal activation is strongly dependent on strain. Klepaczko [16] provided a comprehensive review of physical-based models for metals with different crystal lattice. More recently, Bonora and Milella [17] proposed a semi-empirical constitutive model incorporating damage for predicting both material response and fracture under varying strain rate and temperature conditions. Voyiadjis and Abed [18] developed a physically based yield function for bcc metals. Rusinek and Klepaczko [19] developed a visco-plastic, physically based model, later modified by Rusinek et al. [20] for application in a wide strain rate range. Later, Bonora et al. [21] extended the Rusinek-modified model to simulate deformation of OFHC (oxygen-free high-conductivity) copper under large strain, elevated temperature, and very high strain rate conditions. These are only few examples of an extensive literature. A detailed review of experimental testing and modelling for bcc metals can be found in [22,23] and more recently in [24–26].

However, most of the model formulations are limited to specific temperature and strain rate range. For instance, most of the models address the variation of the yield stress for temperature below 0.2 of the melting temperature T_m where experimental data show the largest temperature effect while very few consider the variation of the yield stress at elevated temperature where deformation process is controlled by diffusion. Similarly, the strain rate effect is often considered only in the range controlled by thermal activation while the regime of the very high strain rates, where viscous effects become dominant, is frequently not considered. Thus, the objective of this paper is to derive physically based constitutive relations for bcc metals over the whole temperature range, from 0 K to T_m, and for strain rate ranging from 10^{-4}/s up to 10^{7}/s considering thermally activated, diffusion controlled, and viscous regimes.

2. Materials and Methods

The temperature and strain rate sensitivity of bcc metals and alloys is considered. For this class of materials, the yield stress shows a strong dependence on the strain rate and temperature while that for the plastic strain hardening is weak or negligible. Such, sensitivity of bcc metals is generally attributed to the rate-controlling mechanisms of thermal component of the flow stress. The yield stress is mainly due to Peierls barriers, and dislocations slip is primarily controlled by high Peierls stress because of the non-planar structure of screw dislocations. Thermal activation helps dislocation glide by reducing the internal friction, facilitating the slip and decreasing the material flow stress. This results in a strong temperature dependence of the flow stress in bcc metals, which implies also a strong dependence on the strain rate. For bcc metals, experimental data indicates a substantial increase of the rate sensitivity at low temperature which is related to the thermally activated Peierls potential [27,28]. It follows that coupling between temperature and strain rate is critical for a correct definition of the transition

between the athermal and thermally activated processes of plastic deformation at low temperature and at high strain rates above room temperature [29]. Based on these premises, a mathematical relationship for the yield stress is derived as follows.

The deformation of a metal beyond the elastic limit requires to activate and move dislocations present in the material through the crystal. Two types of obstacle oppose to dislocations motion: long-range and short-range barriers. The first are due to the structure and cannot be overcome by thermal energy. They supply the flow stress with a contribution that is not thermally activated, usually indicated as athermal stress component. The latter, which may include the Peierls stress, point defects, other dislocations that intersect the slip plane, or substitutional atoms, can be overcome by thermal energy and contribute to determining that part of the flow stress affected by the temperature [17]. At increasing strain rates or dislocation velocities viscous phonon drag becomes dominant [30,31] and the applied stress is high enough to overcome instantaneously the usual dislocation barriers without any aid from thermal fluctuations. Therefore, consistently with dislocation kink-pair theory, the yield stress can be expressed as the sum of three contributions,

$$\sigma_Y\left(\dot{\varepsilon}, T\right) = \sigma_{ath} + \sigma_{ta} + \sigma_{vd} \tag{1}$$

where the subscripts "*ath*," "*ta*," and "*vd*" indicate the athermal, thermally activated, and viscous drag components, respectively [7].

Athermal stress. The athermal stress component of the flow stress arises from the elastic interaction of the dislocations and depends on the temperature only though the weak temperature dependence of the shear modulus [32]. It is a function of the density and distribution of the dislocations, grain sizes and their distribution, as well as the density and distribution of precipitates, substitutional atoms, and other impurities and defects [14]. The athermal stress component of the yield stress can be determined experimentally by means of stress reduction and stress relaxation experiments [33] and it is usually given in the Hall-Petch form in order to account for the grain size effect,

$$\sigma_{ath} = \sigma_0 + \frac{K}{\sqrt{d}} \tag{2}$$

where d is the grain size.

Thermally activated stress. Plastic strain and dislocation density are related by the following simple relationship (Orowan's equation),

$$\dot{\varepsilon} = \rho_m b \overline{v} \tag{3}$$

where $\dot{\varepsilon}$ is the strain rate, b is the Burgers vector, ρ_m is the density of mobile dislocations, and $\overline{v}$ is the average of dislocation velocity. This equation is derived considering that when a dislocation moves, two atoms on sites adjacent across the plane of motion are displaced relative to each other by the Burgers vector b. However, the Orowan's equation holds also for screw and mixed dislocations. Johnston and Gilman [34] provided experimental evidences that the average velocity of mobile dislocations varies with temperature according to,

$$\overline{v} = \overline{v}_0 \exp\left(-\frac{G^*}{kT}\right) \tag{4}$$

Here, k is the Boltzmann's constant and T the temperature, that substituted in Equation (3) leads to:

$$\dot{\varepsilon} = \rho_m b \overline{v}_0 \exp\left(-\frac{G^*}{kT}\right) = \dot{\varepsilon}_0 \exp\left(-\frac{G^*}{kT}\right) \tag{5}$$

which is the rate equation for plastic flow controlled by thermal fluctuations as derived by Taylor [12] where $\dot{\varepsilon}_0$ is a parameter which depends on the dislocation density, vibrational frequency and strain. This equation is assumed as the starting point for the thermodynamical treatment of deformation [35]. G^* is the Gibbs free energy—assuming that the effects of dislocation character and slip on secondary

systems are either subsumed in the pre-exponential term $\dot{\varepsilon}_0$ or ignored—which is strongly affected by the work done by the applied stress during activation. Thus, it can be written as:

$$G^* = G^*(\sigma) \tag{6}$$

Since the stress experienced by dislocation is a combination of the applied resolved stress and stresses from other sources, it is preferred to refer to an effective stress σ^* (i.e., σ_{ta}) defined as:

$$\sigma^* = \sigma_a - \sigma_i \tag{7}$$

where σ_a is the applied stress and σ_i is the internal, or athermal, stress arising from the elastic strain field of other dislocations [36]. Although, the internal stress can be positive or negative when considering the motion of dislocation over short barriers, it always subtract to the applied stress. Therefore, from the rate equation, Equation (6) can be rewritten as,

$$G^*(\sigma^*) = -kT \ln\left(\frac{\dot{\varepsilon}}{\dot{\varepsilon}_0}\right) \tag{8}$$

Therefore, differentiating with respect to effective stress the following expression is obtained:

$$\left(\frac{\partial G^*}{\partial \sigma^*}\right)_T = -kT\left(\frac{\partial \ln\left(\dot{\varepsilon}/\dot{\varepsilon}_0\right)}{\partial \sigma^*}\right)_T \tag{9}$$

This leads to the definition of the activation volume which is given as the negative stress derivative of the activation energy,

$$v^* = -\left(\frac{\partial G^*}{\partial \sigma^*}\right)_T = kT\left(\frac{\partial \ln\left(\dot{\varepsilon}/\dot{\varepsilon}_0\right)}{\partial \sigma^*}\right)_T \tag{10}$$

This form has the advantage with respect to other definitions of v^* of being obtained directly from experiments.

The activation energy cannot be obtained directly from experiments. Recalling that G^* can be written as:

$$G^* = H^* - TS^* \tag{11}$$

where H^* is the activation enthalpy that can be obtained explicitly in differential scanning calorimetry (DSC) tests, and S^* is the activation energy defined as,

$$S^* = -\left(\frac{\partial G^*}{\partial T}\right)_{\sigma^*} \tag{12}$$

Differentiating the rate equation with respect to temperature at constant stress we obtain,

$$\left(\frac{\partial G^*}{\partial T}\right)_{\sigma^*} = -k \ln\left(\frac{\dot{\varepsilon}}{\dot{\varepsilon}_0}\right) - kT\left(\frac{\partial \ln\left(\dot{\varepsilon}/\dot{\varepsilon}_0\right)}{\partial T}\right)_{\sigma^*} \tag{13}$$

At a given temperature, the effective stress and dislocation velocity are related. Therefore, the internal stress differential can be written as,

$$d\sigma^* = \left(\frac{\partial \sigma^*}{\partial T}\right)_{\dot{\varepsilon}/\dot{\varepsilon}_0} dT + \left(\frac{\partial \sigma^*}{\partial \ln\left(\dot{\varepsilon}/\dot{\varepsilon}_0\right)}\right)_T d\ln\left(\frac{\dot{\varepsilon}}{\dot{\varepsilon}_0}\right) \tag{14}$$

Similarly,

$$d\ln\left(\frac{\dot{\varepsilon}}{\dot{\varepsilon}_0}\right) = \left(\frac{\partial \ln\left(\dot{\varepsilon}/\dot{\varepsilon}_0\right)}{\partial T}\right)_{\sigma^*} dT + \left(\frac{\partial \ln\left(\dot{\varepsilon}/\dot{\varepsilon}_0\right)}{\partial \sigma^*}\right)_T d\sigma^* \tag{15}$$

Substituting Equation (15) in Equation (14), we get,

$$\left(\frac{\partial \ln\left(\dot{\varepsilon}/\dot{\varepsilon}_0\right)}{\partial T}\right)_{\sigma^*} = -\left(\frac{\partial \ln\left(\dot{\varepsilon}/\dot{\varepsilon}_0\right)}{\partial \sigma^*}\right)_T \left(\frac{\partial \sigma^*}{\partial T}\right)_{\dot{\varepsilon}/\dot{\varepsilon}_0} \tag{16}$$

and therefore,

$$H^* = kT^2\left(\frac{\partial \ln\left(\dot{\varepsilon}/\dot{\varepsilon}_0\right)}{\partial T}\right)_{\sigma^*} = -kT^2\left(\frac{\partial \ln\left(\dot{\varepsilon}/\dot{\varepsilon}_0\right)}{\partial \sigma^*}\right)_T \left(\frac{\partial \sigma^*}{\partial T}\right)_{\dot{\varepsilon}/\dot{\varepsilon}_0} \tag{17}$$

From this, the internal stress derivative with respect to the temperature at constant deformation rate can be obtained, and recalling the definition of the activation volume, we can finally write,

$$\left(\frac{\partial \sigma^*}{\partial T}\right)_{\dot{\varepsilon}/\dot{\varepsilon}_0} = -\frac{H^*}{kT^2} \Big/ \left(\frac{\partial \ln\left(\dot{\varepsilon}/\dot{\varepsilon}_0\right)}{\partial \sigma^*}\right)_T = -\frac{H^*}{T}\frac{1}{v^*} \tag{18}$$

According to Equation (18), the derivative of the internal stress with respect to temperature, which describes the temperature dependence of the flow stress at constant strain rate, is proportional to the ratio of the activation enthalpy and temperature and activation volume.

The activation volume is a nonlinear function of temperature. In the low temperature range, the activation volume increases with temperature while at elevated temperature, in the diffusion-controlled regime, it decreases with increasing temperature. In order to describe the variation of the activation volume over the whole temperature range, from 0 K to T_m, the following expression is proposed,

$$v^* = \frac{v_0^*}{T_m}\left[\Gamma_{TH}(T) + \Gamma_{DC}(T)\right]^{-1} \tag{19}$$

where the first term in the right square bracket is for the plasticity limited by lattice resistance (thermally activated regime, low temperature) while the latter is for the diffusion-controlled flow (elevated temperature), with

$$\begin{aligned} \Gamma_{TH} &= \tfrac{A}{T_1}\exp\left(-\tfrac{T}{T_1}\right)\exp\left(-\left(\tfrac{T}{T_2}\right)^m\right) \\ \Gamma_{DC} &= \tfrac{m}{T_2}\left(\tfrac{T}{T_2}\right)^{m-1}\left(1 + A\exp\left(-\tfrac{T}{T_1}\right)\right)\exp\left(-\left(\tfrac{T}{T_2}\right)^m\right) \end{aligned} \tag{20}$$

where T_1 and T_2 are the mean temperature of the thermally activated and the diffusion controlled regime, respectively, A and m are dimensionless material constants, T_m is the melting temperature and v_0^* is the activation volume at T_m. Substituting Equation (20) in Equation (19) we finally obtain,

$$v^* = \frac{v_0^*}{T_m}\exp\left(\left(\frac{T}{T_2}\right)^m\right)\left[\frac{A}{T_1}\exp\left(-\frac{T}{T_1}\right) + \frac{m}{T_2}\left(1 + A\exp\left(-\frac{T}{T_1}\right)\right)\left(\frac{T}{T_2}\right)^{m-1}\right]^{-1} \tag{21}$$

Also the activation enthalpy is temperature dependent [37]. In the low temperature range, and for $T < T_1$, a linear relationship can be assumed,

$$H^* = cT \tag{22}$$

where c assumes different values for the thermally activated and for the diffusion-controlled regime. Then, substituting Equation (22) and Equation (21) in Equation (18) we obtain,

$$\left(\frac{\partial \sigma^*}{\partial T}\right)_{\dot{\varepsilon}/\varepsilon_0} = -\frac{cT_m}{v_0^*}\exp\left(-\left(\frac{T}{T_2}\right)^m\right)\left[\frac{A}{T_1}\exp\left(-\frac{T}{T_1}\right) + \frac{m}{T_2}\left(1 + A\exp\left(-\frac{T}{T_1}\right)\right)\left(\frac{T}{T_2}\right)^{m-1}\right] \tag{23}$$

Thus, Equation (14) can be rewritten as,

$$d\sigma^* = -\frac{H^*}{T}\frac{1}{v^*}dT + \frac{kT}{v^*}d\ln\left(\frac{\dot{\varepsilon}}{\dot{\varepsilon}_0}\right) \tag{24}$$

that substituting the expression for the activation volume, integrating and grouping common factors leads to

$$\sigma^* = \frac{cT_m}{v_0^*}\Delta_1\Delta_2\left\{1 + \frac{k}{c}\ln\left(\frac{\dot{\varepsilon}}{\dot{\varepsilon}_0}\right)\left[m\left(\frac{T}{T_2}\right)^m + \frac{T}{T_1}\left(1 - \frac{1}{\Delta_1}\right)\right]\right\} \tag{25}$$

where

$$\begin{array}{c} \Delta_1 = 1 + A\exp\left(-\frac{T}{T_1}\right) \\ \Delta_2 = \exp\left(-\left(\frac{T}{T_2}\right)^m\right) \end{array} \tag{26}$$

In Equation (25) the stress contribution given by the second term in the square bracket is small compared to that of the first term, and in a first approximation, can be neglected. Therefore, we can write

$$\sigma^* = \sigma_{th}^0\Delta_1\Delta_2\left\{1 + \lambda\ln\left(\frac{\dot{\varepsilon}}{\dot{\varepsilon}_0}\right)\right\} \tag{27}$$

where

$$\begin{array}{c} \sigma_{th}^0 = \frac{cT_m}{v_0^*} \\ \lambda = \frac{k}{c}m\left(\frac{T}{T_2}\right)^m \end{array} \tag{28}$$

where σ_{th}^0 is a fraction of the thermal stress at 0 K (which is $\sigma_{th}^0(1 + A)$) and λ is the strain rate sensitivity parameter.

Viscous drag stress. At low strain rates in the thermally activated region, the viscous drag component is negligible. It becomes more and more relevant at increasing the strain rate. In the viscous drag-dominated regime the yield stress is a linear function of the strain rate. Here, the following simple expression is proposed,

$$\sigma_{vd} = \sigma_{vd}^0\left[\frac{\dot{\varepsilon}}{\dot{\varepsilon}_0} - 1\right] \tag{29}$$

where σ_{vd} is a scale factor.

Finally, combining Equation (2), Equation (27), and Equation (29) the following expression for the constitutive equation is obtained,

$$\sigma^* = \sigma_0 + \frac{K}{\sqrt{d}} + \sigma_{th}^0\left(1 + A\exp\left(-\frac{T}{T_1}\right)\right)\exp\left(-\left(\frac{T}{T_2}\right)^m\right)\left\{1 + \lambda\ln\left(\frac{\dot{\varepsilon}}{\dot{\varepsilon}_0}\right)\right\} + \sigma_{vd}^0\left[\frac{\dot{\varepsilon}}{\dot{\varepsilon}_0} - 1\right] \tag{30}$$

Formally, the model requires ten parameters that can be identified from experimental data at different strain rate and temperature. However, they can be reduced to eight if the athermal stress is assumed as a single parameter. In the present formulation, the reference strain rate $\dot{\varepsilon}_0$ is the strain rate at which transition between the athermal and thermally activated regime occurs. In bcc metals, this is also temperature dependent as clearly shown by Campbell and Ferguson [38] for mild steel.

Here, the following expression for the temperature dependence of the transition strain rate in bcc is proposed,

$$\dot{\varepsilon}_0 = \dot{\varepsilon}_{vd}\left(\frac{T}{T_m}\right)^m \tag{31}$$

where $\dot{\varepsilon}_{vd}$ is the strain rate limit for the domain of validity of the linear viscous drag law [39].

3. Results

The proposed model has been validated predicting the yield stress at different strain rates and temperature for A508 steel (equivalent to 16MND5). This is a low alloyed steel with bcc atomic structure, developed for reactor pressure vessel applications. The microstructure is a restored bainite and the ferritic matrix is reinforced by carbides (of the order of 1 µm) resulting from the precipitation of cementite, upper and lower (spheroids) bainite together with several types of inclusions manganese sulphide (MnS). The reference composition is given in Table 1 [35].

Table 1. Chemical composition of A508 steel.

Element	C	S	P	Si	Mn	Ni	Cr	Mo	Cu	Co
wt.%	0.16	0.005	0.006	0.19	1.35	0.74	0.18	0.51	0.007	0.01

Experimental data at different temperature and strain rates were taken from different sources [40–42].

Identification of model parameters has been performed as follow. First, non-linear fitting of yield stress data as a function of temperature, for the nominal strain rate of 10^{-4}/s, was performed using Equation (30) neglecting the contribution of the viscous drag. Here, the athermal stress was treated as a single parameter. As a result of this procedure σ_{ath}, σ^0_{th}, A, T_1, T_2, and m were determined. Second, the remaining model parameters, λ, σ^0_{vd} were determined by fitting yield stress data as a function of the strain rate for T = 293 K. T_m is given for the material under investigation and $\dot{\varepsilon}^0_{vd}$ is taken as 10^6/s.

In Figure 1, the comparison of the present model solution (fitted) for the yield stress as a function of temperature and experimental the data is given. In Figure 2, the predicted yield stress as a function of the strain rate at different temperature is shown.

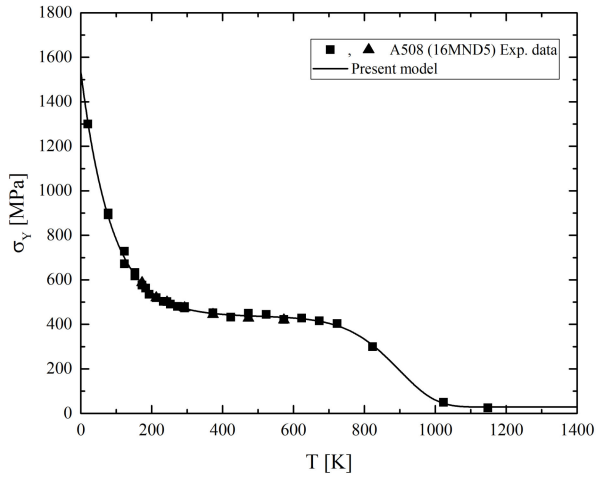

Figure 1. Yield stress as a function of temperature for A508 steel at nominal quasi-static strain rate (10^{-4}/s): result of fitting experimental data with Equation (30).

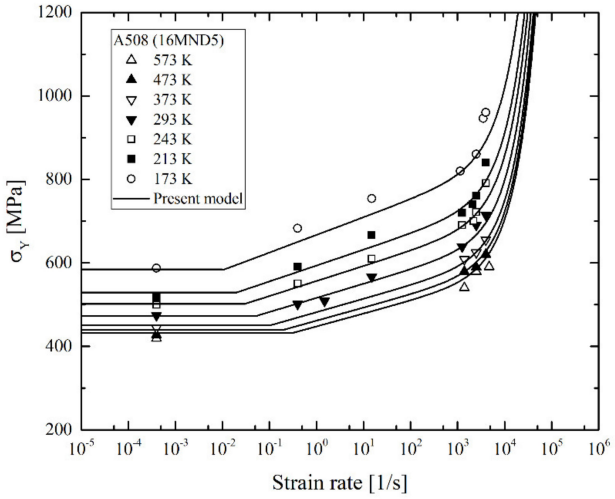

Figure 2. Yield stress of A508 steel as a function strain at different temperature. Here, only data at T = 293 K were used to fit the material model parameters while for other temperatures the behavior predicted by present model solution is shown.

Finally, material model parameters for A508 steel are summarized in Table 2.

Table 2. Model parameters for A508 steel.

Parameter	σ_{ath}[MPa]	σ^0_{th}[MPa]	A	T_1 [K]	T_2 [K]	m	λ	T_m [K]	$\dot{\varepsilon}^0_{vd}$[1/s]	σ^0_{vd} [MPa]
Value	28.7	407.0	2.7	86.5	908.5	9.83	0.033	1623	10^6	5×10^{-3}

4. Conclusions

In this work a physically based model for the yield stress in bcc has been developed based on dislocations mechanics and according to a thermodynamical treatment of deformation. Although the approach for physically based model is well established in the literature, in the present paper the expression for the temperature activation volume, which is highly nonlinear over the whole temperature range, predicts the coupling between strain rate and temperature effect in the thermally activated regime of the yield stress. In addition, predicted strain rate effect, $1 + \lambda \ln\left(\dot{\varepsilon}/\dot{\varepsilon}_0\right)$, is found consistent with that of the Johnson and Cook of phenomenological derivation, providing a physical meaning to the scale factor $\dot{\varepsilon}_0$ that here is the strain rate at which the thermal activation effect becomes dominant over the athermal stress component, with $\dot{\varepsilon}_0$ being temperature dependent.

Author Contributions: Conceptualization G.T., N.B.; methodology, N.B.; validation, A.R.; data analysis, G.I. and G.T.; investigation, G.T.; writing—original draft preparation, N.B.; writing—review and editing, G.T. and N.B. All authors have read and agreed to the published version of the manuscript.

Funding: This research received no external funding.

Conflicts of Interest: The authors declare no conflict of interest.

References

1. Kuehmann, C.J.; Olson, G.B. Computational materials design and engineering. *Mater. Sci. Technol.* **2009**, *25*, 472–478. [CrossRef]
2. Allen, D.H.; Harris, C.E. *A Review of Nonlinear Constitutive Models for Metals*; Langley Research Center: Hampton, VA, USA, 1990.
3. Bodner, S.R. Review of a unified elastic—Viscoplastic theory. In *Unified Constitutive Equations for Creep and Plasticity*; Springer: Dordrecht, The Netherlands, 1987; pp. 273–301. [CrossRef]

4. Cowper, G.R.; Symonds, P.S. *Strain-Hardening and Strain-Rate Effects in the Impact Loading of Cantilever Beams*; Brown University: Providence, RI, USA, 1957.
5. Johnson, G.R.; Cook, W.H. Fracture characteristics of three metals subjected to various strains, strain rates, temperatures and pressures. *Eng. Fract. Mech.* **1985**, *21*, 31–48. [CrossRef]
6. Bodner, S.R.; Partom, Y. Constitutive equations for elastic-viscoplastic strain-hardening materials. *J. Appl. Mech.* **1975**, *42*, 385–389. [CrossRef]
7. Nemat-Nasser, S.; Li, Y. Flow stress of fcc polycrystals with application to OFHC Cu. *Acta Mater.* **1998**, *46*, 565–577. [CrossRef]
8. Surek, T.; Luton, M.; Jonas, J. Dislocation glide controlled by linear elastic obstacles: A thermodynamic analysis. *Philos. Mag. A J. Theor. Exp. Appl. Phys.* **1973**, *27*, 425–440. [CrossRef]
9. Kocks, U.; Argon, A.; Ashby, M. Thermodynamics and kinetics of slip. *Prog. Mater. Sci.* **1975**, *19*, 1–281.
10. Follansbee, P.; Kocks, U. A constitutive description of the deformation of copper based on the use of the mechanical threshold stress as an internal state variable. *Acta Metall.* **1988**, *36*, 81–93. [CrossRef]
11. Voyiadjis, G.Z.; Abed, F.H. Microstructural based models for bcc and fcc metals with temperature and strain rate dependency. *Mech. Mater.* **2005**, *37*, 355–378. [CrossRef]
12. Taylor, G. Thermally-activated deformation of BCC metals and alloys. *Prog. Mater. Sci.* **1992**, *36*, 29–61. [CrossRef]
13. Cosrad, H. Effect of temperature on yield and flow stress of BCC metals. *Philos. Mag.* **1960**, *5*, 745–751. [CrossRef]
14. Kawata, K.; Hashimoto, S.; Kurokawa, K. Analyses of high velocity tension of bars of finite length of BCC and FCC metals with their own constitutive equations. In *High Velocity Deformation of Solids*; Springer: Berlin/Heidelberg, Germany, 1979; pp. 1–15.
15. Zerilli, F.J.; Armstrong, R.W. Dislocation-mechanics-based constitutive relations for material dynamics calculations. *J. Appl. Phys.* **1987**, *61*, 1816–1825. [CrossRef]
16. Klepaczko, J.R. Constitutive modeling in dynamic plasticity based on physical state variables-A review. *Le Journal de Physique Colloques* **1988**, *49*, C3-553–C3-560. [CrossRef]
17. Bonora, N.; Milella, P.P. Constitutive modeling for ductile metals behavior incorporating strain rate, temperature and damage mechanics. *Int. J. Impact Eng.* **2001**, *26*, 53–64. [CrossRef]
18. Voyiadjis, G.Z.; Abed, F.H. A coupled temperature and strain rate dependent yield function for dynamic deformations of bcc metals. *Int. J. Plast.* **2006**, *22*, 1398–1431. [CrossRef]
19. Rusinek, A.; Klepaczko, J. Shear testing of a sheet steel at wide range of strain rates and a constitutive relation with strain-rate and temperature dependence of the flow stress. *Int. J. Plast.* **2001**, *17*, 87–115. [CrossRef]
20. Rusinek, A.; Rodríguez-Martínez, J.A.; Arias, A. A thermo-viscoplastic constitutive model for FCC metals with application to OFHC copper. *Int. J. Mech. Sci.* **2010**, *52*, 120–135. [CrossRef]
21. Bonora, N.; Testa, G.; Ruggiero, A.; Iannitti, G.; Mortazavi, N.; Hörnqvist, M. Numerical simulation of dynamic tensile extrusion test of ofhc copper. *J. Dyn. Behav. Mater.* **2015**, *1*, 136–152. [CrossRef]
22. Liang, R.; Khan, A.S. A critical review of experimental results and constitutive models for BCC and FCC metals over a wide range of strain rates and temperatures. *Int. J. Plast.* **1999**, *15*, 963–980. [CrossRef]
23. Khan, A.S.; Liang, R. Behaviors of three BCC metal over a wide range of strain rates and temperatures: Experiments and modeling. *Int. J. Plast.* **1999**, *15*, 1089–1109. [CrossRef]
24. Huh, H.; Ahn, K.; Lim, J.H.; Kim, H.W.; Park, L.J. Evaluation of dynamic hardening models for BCC, FCC, and HCP metals at a wide range of strain rates. *J. Mater. Process. Technol.* **2014**, *214*, 1326–1340. [CrossRef]
25. Salvado, F.C.; Teixeira-Dias, F.; Walley, S.M.; Lea, L.J.; Cardoso, J.B. A review on the strain rate dependency of the dynamic viscoplastic response of FCC metals. *Prog. Mater. Sci.* **2017**, *88*, 186–231. [CrossRef]
26. Gray III, G.T. High-strain-rate deformation: Mechanical behavior and deformation substructures induced. *Annu. Rev. Mater. Res.* **2012**, *42*, 285–303. [CrossRef]
27. Conrad, H. Thermally activated deformation of metals. *JOM* **1964**, *16*, 582–588. [CrossRef]
28. Klepaczko, J. A general approach to rate sensitivity and constitutive modeling of FCC and BCC metals. *Impact Eff. Fast Transient Load.* **1988**, 3–35.
29. Rusinek, A.; Zaera, R.; Klepaczko, J.R. Constitutive relations in 3-D for a wide range of strain rates and temperatures–application to mild steels. *Int. J. Solids Struct.* **2007**, *44*, 5611–5634. [CrossRef]
30. Kumar, A.; Hauser, F.; Dorn, J. Viscous drag on dislocations in aluminum at high strain rates. *Acta Metall.* **1968**, *16*, 1189–1197. [CrossRef]

31. Vreeland, T., Jr.; Lau, S. *Study of Dislocation Mobility and Density in Metallic Crystals*; Technical report; WM Keck Lab. of Engineering Materials; California Institute of Technology: Pasadena, CA, USA, 1974.
32. Nabarro, F.R.; Duesbery, M.S. *Dislocations in Solids*; Elsevier: Amsterdam, The Netherlands, 2002; Volume 11.
33. Kruml, T.; Coddet, O.; Martin, J. About the determination of the thermal and athermal stress components from stress-relaxation experiments. *Acta Mater.* **2008**, *56*, 333–340. [CrossRef]
34. Johnston, W.G.; Gilman, J.J. Dislocation velocities, dislocation densities, and plastic flow in lithium fluoride crystals. *J. Appl. Phys.* **1959**, *30*, 129–144. [CrossRef]
35. Vineyard, G.H. Frequency factors and isotope effects in solid state rate processes. *J. Phys. Chem. Solids* **1957**, *3*, 121–127. [CrossRef]
36. Tanibayashi, M. A Method to Determine the Internal Stress and the Stress Exponent m of the Dislocation Velocity. *Phys. Status Solidi (A)* **1990**, *120*, K19–K23. [CrossRef]
37. Arsenault, R.; Li, J.C. Thermally activated dislocation motion in a periodic internal stress field. *Philos. Mag. A J. Theor. Exp. Appl. Phys.* **1967**, *16*, 1307–1311. [CrossRef]
38. Campbell, J.; Ferguson, W. The temperature and strain-rate dependence of the shear strength of mild steel. *Philos. Mag.* **1970**, *21*, 63–82. [CrossRef]
39. Gurrutxaga-Lerma, B.; Balint, D.; Dini, D.; Sutton, A. The mechanisms governing the activation of dislocation sources in aluminum at different strain rates. *J. Mech. Phys. Solids* **2015**, *84*, 273–292. [CrossRef]
40. Tanguy, B.; Besson, J.; Piques, R.; Pineau, A. Ductile to brittle transition of an A508 steel characterized by Charpy impact test: Part II: Modeling of the Charpy transition curve. *Eng. Fract. Mech.* **2005**, *72*, 413–434. [CrossRef]
41. Chapuliot, S.; Lacire, M.; Marie, S.; Nédélec, M. Thermomechanical analysis of thermal shock fracture in the brittle/ductile transition zone. Part I: Description of tests. *Eng. Fract. Mech.* **2005**, *72*, 661–673. [CrossRef]
42. Reytier, M.; Chapuliot, S.; Marie, S.; Ferry, L.; Nedelec, M. Study of cleavage initiation under thermal shock by tests on cracked rings and thermomechanical calculations. *Nucl. Eng. Des.* **2006**, *236*, 1039–1050. [CrossRef]